Can $\langle P_4 \rangle$ Be Obtained from Fluorescence Depolarization in Liquid Crystals?

I. – Rodlike Probes (*)(**).

A. ARCIONI, R. TARRONI and C. ZANNONI

Dipartimento di Chimica Fisica ed Inorganica dell'Università
Viale Risorgimento 4, 40136 Bologna, Italia

(ricevuto l'1 Agosto 1988)

Summary. — We have investigated the possibility of obtaining the fourth-rank orientational order parameter $\langle P_4 \rangle$ for a rodlike probe molecule dissolved in a liquid crystal from a time-dependent fluorescence depolarization experiment. Simulated data at various temperatures have been prepared and then analysed both individually and simultaneously using the previously proposed «global target» deconvolution approach. We have examined, in particular, the case of a pure $P_4(\cos\beta)$ effective potential. Approximate solutions of the diffusion equation recently put forward in the literature have also been tested.

PACS 61.30 – Liquid crystals.
PACS 64.70 – Phase equilibria, phase transitions and critical points of specific substances.
PACS 87.30 – Biophysics of neurophysiological processes (excluding perception processes and speech).

1. – Introduction.

A particularly appealing characteristic of the fluorescence depolarization technique is that of being able to provide, at least in principle, not only second-

(*) To speed up publication, the authors of this paper have agreed to not receive the proofs for correction.
(**) Work presented at the First USSR-Italy Bilateral Meeting on Liquid Crystals held in Portonovo, Ancona (Italia), September 30 - October 2, 1987.

rank, but also fourth-rank order parameters [1]. Theory predicts that what can be obtained from a certain experiment will depend on the relative time scales of the fluorescence decay and reorientation processes τ_F and τ_R. A classical example is that of a rodlike probe molecule with absorption and emission transition moments [2] μ and $\bar{\mu}$ parallel to the long molecular axis and dissolved in an oriented mesophase [1,3]. In an idealized experiment the initial time anisotropy depends both on $\langle P_2 \rangle$ and on $\langle P_4 \rangle$. Thus we expect that the fourth-rank order parameter $\langle P_4 \rangle$ for the probe can be obtained when the fluorescence time decay τ_F is somewhat shorter than the long axis correlation time τ_{00}, so that the initial decay is effectively sampled and provided that $\langle P_2 \rangle$ can be determined as well. On the other hand, if τ_F is much longer than τ_{00}, so that the photoselected molecules have time to relax to orientational equilibrium, only the second-rank Legendre polynomial average $\langle P_2 \rangle$ can be reliably obtained. The maximum amount of information can be extracted from experiments where the time evolution of fluorescence depolarization is followed [3,4].

There, in fact, the time dependence of the long axis orientational correlation functions can potentially be obtained from the time dependence of the polarization anisotropy after a very short excitation pulse [5]. For a probe with arbitrary orientation of the absorption and emission transition moments various linear combinations of orientational correlation functions contribute to the observable intensities. Experimental and data analysis problems make the situation more complex. The obtainment of molecular parameters with single-photon counting apparatus normally requires a delicate deconvolution procedure [6,7]. Even with faster response apparatus [5] accessing the initial part of the decay is troublesome. I the present paper we wish to investigate the question of the amount of molecular information that can actually be extracted from experimental data. Thus we shall construct sets of simulated data representative of a few important experimental conditions and analyse them with various procedures.

2. – Theory.

2·1. *Resumé of fluorescence depolarization theory.* – The basic theory of fluorescence depolarization in liquid crystals has been described in detail

---

[1] C. ZANNONI: *Mol. Phys.*, **38**, 1813 (1979).
[2] J. MICHL and E. W. THULSTRUP: *Spectroscopy with Polarized Light*, VCH (1987).
[3] C. ZANNONI, A. ARCIONI and P. CAVATORTA: *Chem. Phys. Lipids*, **32**, 179 (1983).
[4] A. ARCIONI, F. BERTINELLI, R. TARRONI and C. ZANNONI: *Mol. Phys.*, **61**, 1161 (1987).
[5] E. V. GORDEEV, V. K. DOLGANOV and V. V. KORSHUNOV: *JETP Lett.*, **43**, 766 (1986).
[6] A. ARCIONI and C. ZANNONI: *Chem. Phys.*, **88**, 113 (1984).
[7] R. B. CUNDALL and R. E. DALE (Editors): *Time Resolved Fluorescence Spectroscopy in Biochemistry and Biology* (Plenum Press, New York, N. Y., 1983).

elsewhere ([1,4]). Here we just wish to recall the bare minimum necessary to establish notation and to prepare the ground for the data analysis section. We start by defining the geometry of the experiment as having the uniformly aligned liquid-crystal sample placed at the origin. We assume the Z-axis parallel to this monodomain preferred orientation (the director) and the exciting light to be coming along the laboratory Y direction with polarization direction $\boldsymbol{e}_i$. The fluorescent probe has effective cylyndrical symmetry, *i.e.* we assume that its ordering matrix cannot be distinguished from a truly uniaxial one. The transition moments μ and $\bar{\mu}$ can possibly be tilted away from the effective symmetry axis with Cartesian components

$$\mu = |\mu|(0, 0, \cos\beta_a)\,, \tag{1}$$

$$\bar{\mu} = |\bar{\mu}|(\sin\beta_e\,, \cos\alpha_e \sin\beta_e \sin\alpha_e\,, \cos\beta_e)\,, \tag{2}$$

where β_a, α_e, β_e give the transition moments orientation in the molecule fixed frame. The dye concentration is assumed to be so low that probe-probe intermolecular relaxation effects can be neglected and the pulse intensity to be weak enough to avoid saturation effects ([8]). Fluorescence light is observed in the forward or in the right angle direction through an analyser, set at a direction of polarization $\boldsymbol{e}_f$. The theory can of course be adapted with straightforward modifications to any other observation geometry. The relevant fluorescence intensities at a time t after an instantaneous excitation pulse can be written, when reorientation is the dominant depolarization mechanism and the fluorescence and reorientation processes are statistically independent, as

$$I_{ZZ}(t)/F(t) = \frac{1}{9} + \frac{2}{9}\langle P_2\rangle[P_2(\cos\beta_a) + P_2(\cos\beta_e)] + \\ + \frac{4}{9}\sum_n D^{2*}_{n0}(0\,\beta_a\,0)\, D^2_{n0}(\alpha_e\beta_a 0)\, \phi_{0n}(t)\,, \tag{3}$$

$$I_{ZX}(t)/F(t) = \frac{1}{9} + \frac{1}{9}\langle P_2\rangle[2P_2(\cos\beta_a) - P_2(\cos\beta_e)] - \\ - \frac{2}{9}\sum_n D^{2*}_{n0}(0\,\beta_a\,0)\, D^2_{n0}(\alpha_e\beta_e 0)\, \phi_{0n}(t)\,, \tag{4}$$

where $D^L_{ab}(\alpha\beta\gamma)$ is a Wigner rotation matrix ([9]) and the second-rank orientational correlation functions $\phi_{qn}(t)$, defined as an average over the molecular orientations ω_0, ω_t at time zero and a time t,

$$\phi_{qn}(t) = \langle D^2_{qn}(\omega_0)\, D^{2*}_{qn}(\omega_t)\rangle\,, \tag{5}$$

([8]) K. RAZI-NAQVI: *J. Chem. Phys.*, 73, 3019 (1980).
([9]) M. E. ROSE: *Elementary Theory of Angular Momentum* (Wiley, New York, N. Y., 1957).

describe the rotational dynamics of the probe. We shall also employ the fluorescence anisotropy ratio

$$r(t) = \frac{I_{ZZ}(t) - I_{ZX}(t)}{I_{ZZ}(t) + 2I_{ZX}(t)}. \tag{6}$$

When a probe has effective cylindrical symmetry, the order parameters that can be obtained are at the most $\langle P_2 \rangle$ and $\langle P_4 \rangle$. Thus the most general singlet orientational distribution $f(\beta)$ we can infer from such an experiment has, according to maximum entropy principles [10], the form [11]

$$f(\beta) = \exp\left[a_0 + a_2 P_2(\cos\beta) + a_4 P_4(\cos\beta)\right], \tag{7}$$

where a_0 is determined from the normalization condition of $f(\beta)$ and at each temperature a_2, a_4 should give back the experimental $\langle P_2 \rangle$, $\langle P_4 \rangle$.

In practice what is actually observed is a set of intensities and we will try to fit them to a theoretical model based on the distribution in eq. (7). In particular, the computation of theoretical intensities is based on assuming a rotational diffusion model for the reorientation of the molecules in the anisotropic potential

$$-U_{\text{probe}}(\beta)/kT = a_2 P_2(\cos\beta) + a_4 P_4(\cos\beta). \tag{8}$$

Thus a rotational diffusion equation can be set up in the usual way [12] and orientational autocorrelation functions can be calculated. No additional approximation is really needed. However, various authors [13-15] then proceed to a drastic approximation of the orientational autocorrelation functions, writing them in terms of their first few time derivatives. It is not clear, in general, if additional errors are introduced in this way and what they amount to. In the appendix we shall examine this point. In the rest of this paper we shall always use the full numerical solution.

---

[10] R. D. LEVINE and M. TRIBUS (Editors): *The Maximum Entropy Formalism* (MIT Press, 1979).

[11] R. P. H. KOOYMAN, Y. K. LEVINE and B. W. VAN DER MEER: *Chem. Phys.*, **60**, 317 (1981).

[12] P. L. NORDIO and U. SEGRE: *The Molecular Physics of Liquid Crystals*, edited by G. R. LUCKHURST and G. W. GRAY (Academic Press, New York, N. Y., 1979), Chapt. 18, p. 411.

[13] B. W. VAN DER MEER, H. POTTEL, W. HERREMAN, M. AMELOOT, H. HENDRICKX and H. SCHRODER: *Biophys. J.*, **46**, 515 (1984).

[14] M. AMELOOT, H. HENDRICKX, W. HERREMAN, H. POTTEL, F. VAN CAUWELAERT and W. VAN DER MEER: *Biophys. J.*, **46**, 525 (1984).

[15] L. BEST, E. JOHN, F. JÄHNIG: *Eur. J. Biophys.*, **15**, 87 (1987).

3. – Preparation of temperature-dependent simulated data.

The question of the amount of molecular information obtainable is in general not an easy one to answer and is complicated by deconvolution. In ref. ([6,16]) we have approached the problem using a simulation technique. The general idea is to prepare theoretical intensity curves using eqs. (3), (4) we have seen earlier and an assumed instrument function. Then Poisson noise to a predetermined level is added. The data obtained in this way are treated as true experimental data and analysed to see if the molecular parameters can be recovered for those simulated conditions. We are also interested in exploring the possible advantages of the global target analysis (GTA) procedure ([4]) where data from different temperatures are simultaneously analysed. Thus we have first devised a way of preparing a set of plausible simulated data at various temperatures. To this end we have assumed that the probe is experiencing rotational diffusion in an effective potential as given by the Humphries-James-Luckhurst molecular field theory for second- and fourth-rank interactions between solute and solvent ([17,18]). This $P_2 - P_4$ potential is

$$-U_{\text{probe}}(\beta) = u_2 \langle P_2 \rangle_{\text{solv}} P_2(\cos\beta) + u_4 \langle P_4 \rangle_{\text{solv}} P_4(\cos\beta), \tag{9}$$

where u_2, u_4 are solute-solvent interaction coefficients and $\langle P_L \rangle_{\text{solv}}$ are pure solvent order parameters. The pure solvent order parameters are in turn obtained assuming that a Humpries-James-Luckhurst ([17]) mean field applies to the pure nematic, *i.e.*

$$-U_{\text{solv}}(\beta) = c_2[\langle P_2 \rangle_{\text{solv}} P_2(\cos\beta) + \lambda_{\text{solv}} \langle P_4 \rangle_{\text{solv}} P_4(\cos\beta)], \tag{10}$$

where c_2 is a solvent-solvent interaction energy and λ_{solv} is the ratio between the fourth-rank and second-rank interaction coefficients. The solvent order parameter $\langle P_2 \rangle_{\text{solv}}$, $\langle P_4 \rangle_{\text{solv}}$ obey self-consistency equations and follow from mean field theory. They are defined at a certain temperature T when a nematic-isotropic transition temperature T_{NI} is assigned. As a special case the Maier-Saupe solvent potential is obtained when $\lambda_{\text{solv}} = 0$. The perpendicular component of the diffusion tensor $D_\perp$ at the various temperatures has been assumed to follow an Arrhenius-type behaviour ([4])

$$D_\perp(T) = D_\perp^0 \exp[-E_a/RT], \tag{11}$$

([16]) A. ARCIONI, R. TARRONI and C. ZANNONI: *New Developments in Polarized Spectroscopy of Ordered Systems*, edited by B. SAMORÌ and E. THULSTRUP (Reidel, 1988).

([17]) R. L. HUMPHRIES, P. G. JAMES and G. R. LUCKHURST: *J. Chem. Soc. Faraday Trans. II*, **68**, 1031 (1972).

([18]) G. R. LUCKHURST and M. SETAKA: *Mol. Cryst. Liq. Cryst.*, **19**, 279 (1973).

where E_a is an activation energy. An extensive set of simulations and analysis has been performed and will be reported in the next section. We shall use the Maier-Saupe limit for the solvent potential, although the full form eq. (10) will be used in the analysis. We have convoluted the theoretical intensities I_{ij} with instrumental function as described in [6,16]. The pulse function employed is [6,19]

$$P(t) = at^3 \exp[-t] \tag{12}$$

with a determining the count level. Typical count levels used for $I_{\parallel} + 2I_{\perp}$ were between 30 kcounts and 80 kcounts at the peak level, *i.e.* in a range of values obtainable with an ordinary single-photon apparatus. We consider intensity histograms over 256 channels with a width of 0.1 ns. We also include scattered light, as a fraction of the pulse, on the parallel (10%) and on the perpendicular channel (1%) and a time shift of 0.1 ns. We have considered rodlike probes dissolved in an oriented phase made up of elongated particles and a few typical transition moment geometries. The fluorescence of the probe is assumed to decay exponentially with a fluorescence time $\tau_F = 6$ ns.

4. – Data analysis.

We have employed four different strategies

4·1. *Individual target analysis* (ITA) *for each temperature.* – This is the most straightforward procedure. It consists in analysing each temperature on its own. We have called target analysis the procedure of doing deconvolution not to a sum of free exponentials but rather to the parameters in in the model employed (here the diffusional one) [6,20]. Target analysis [6] is performed on each set of data to determine in particular $a_2(T)$, $a_4(T)$ in eq. (8) and $D_{\perp}(T)$. We also employ the results of this analysis as a guideline for starting the global procedures described in what follows.

4·2. *Diffusion tensor globalization* (DTGA). – We have also performed a diffusion tensor globalization by assuming an Arrhenius-type law for the component of the probe rotational diffusion tensor $\boldsymbol{D}$ perpendicular to the long axis in [4]. Thus we still determine $a_2(T)$, $a_4(T)$ and we optimize $D_{\perp}^0$ and the activation energy E_a in an equation like eq. (11). Here we have only used a special case of the model with $a_4 = 0$.

---

[19] A. Mc Kinnon, A. G. Szabo and D. R. Miller: *J. Phys. Chem.*, **81**, 1564 (1977).
[20] C. Zannoni: *Theory of Fluorescence Polarization Anisotropy*, in *NATO-ASI on Excited State Probes in Biochemistry and Biology, Acireale, 1984*, directed by A. G. Szabo and L. Masotti.

4·3. *Humphries-James-Luckhurst globalization.* – This is a global fit to the Humphries-James-Luckhurst (HJL) parameters u_2/k, u_4/k, λ_{solv} in eqs. (9), (10) and to $D_\perp^0$ and E_a as before. In principle, it is just a check more than anything else, since we have constructed the data using these very equations, so that we should have $a_2 = u_2 \langle P_2 \rangle_{\text{solv}}/kT$, $a_4 = u_4 \langle P_4 \rangle_{\text{solv}}/kT$. In practice, however, it is a useful test of the feasibility of the complex nonlinear fit problem we have set up.

4·4. *Parabolic global target analysis.* – In many practical situations a reasonable theoretical expression for fitting the relative fourth-rank and second-rank contributions will not be known. Thus the only alternative would seem to perform individual analysis or at most a diffusion tensor globalization. On the other hand, we believe we still have some information on the behaviour of a_2, a_4 in eq. (7) or equivalently of the probe order parameter $\langle P_2 \rangle$, $\langle P_4 \rangle$ as a function of temperature. In particular, we believe that, within the nematic or the isotropic phase, they will fall on a continuous and differentiable curve, and possibly a smooth one. Obviously we know nothing, *a priori*, on this dependence. On the other hand, analysing the various temperature results independently would not implement the simple but important mathematical constraints we just mentioned. A possible approach is to assume an empirical form for $a_4(T)$ which is flexible enough to accommodate every realistic variation that can take place in the data. The simplest choice is to take a simple polynomial or truncated Taylor expansion starting from the lowest temperature T_{min}. Thus we have assumed a simple quadratic dependence for the temperature variation of a_4:

$$a_4(T) = \lambda_0 + \lambda_1 (T - T_{\text{min}}) + \lambda_2 (T - T_{\text{min}})^2 , \tag{13}$$

where λ_0, λ_1, λ_2 are to be determined globally. Notice that no particular physical significance is attached at the moment to the coefficients. We emphasize that the aim is to introduce the requisite of the order parameters as a function of temperature as a means of connecting measurements at different temperatures. In this approach the parameter $a_2(T)$ is individually determined, while $D_\perp$ is globalized as in 4·2.

5. – Results.

5·1. *P_2 potential.* – The first example we consider is that of a probe subject to a pure P_2 probe potential ($u_2/k = 1800$ K, $u_4/k = 0$ K in eq. (9)) with the solvent potential U_{solv} itself being of the Maier-Saupe type ($\lambda_{\text{solv}} = 0$). A count level parameter $a = 30\,000$ (cf. eq. (12)) has been used. We have considered the case of absorption and emission moments parallel or tilted with respect to the long axis and we have prepared simulated intensities at ten temperatures regularly spaced between 60° C and the nematic-isotropic transition temperature 150° C.

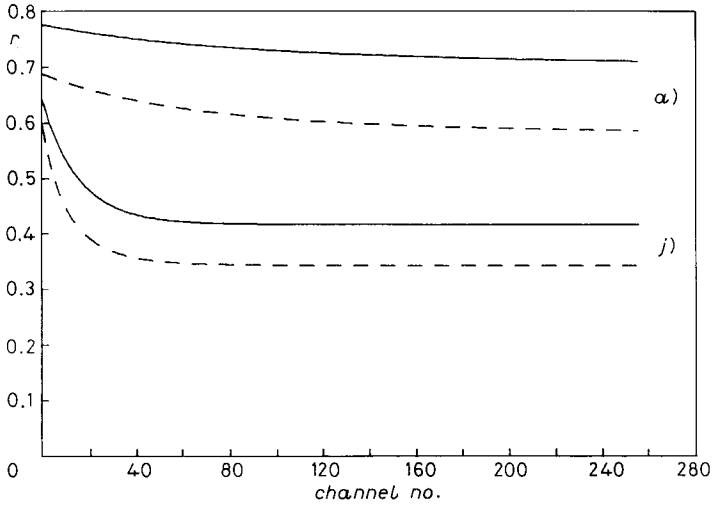

Fig. 1. – Simulated anisotropies $r(t)$ for a rodlike probe in a P_2 potential (eq. (9) with coefficients $u_2/k = 1800\,\mathrm{K}$, $u_4/k = 0\,\mathrm{K}$) in a uniaxial nematic with effective potential, eq. (10) and $T_{\mathrm{NI}} = 150\,^{\circ}\mathrm{C}$. Here $D_{\perp}^{0} = 800\,\mathrm{ns}^{-1}$ and $E_a = 31.4\,\mathrm{kJ/mol}$. The curves are calculated for transition moments μ and $\bar{\mu}$ parallel to the long molecular axis (continuous line) or tilted 20° (dashed line) at temperatures $T = 60.0\,^{\circ}\mathrm{C}$ (a)) and $T = 150.0\,^{\circ}\mathrm{C}$ (j)). Time channel widths is 0.1 ns.

The same temperature grid has been used in all cases treated in this paper. In fig. 1 we show the theoretical anisotropy ratio $r(t)$, eq. (6) at the lowest and highest temperature studied, both for transition moments parallel to the rod axis (continuous line) and for the case of moments parallel to each other but tilted 20° from the molecule axis, to be examined later. We analyzed the data with the $P_2 - P_4$ model, with the aim of seeing if the procedure employed can detect the absence of a fourth-rank term or if the fitting will incorrectly adapt to a nonzero value of the fourth-rank contribution.

In fig. 2 we summarize the results of the different analyses as follows. First we report at the top the input values of $\langle P_2 \rangle$ and $\langle P_4 \rangle$ (fig. 2a)) and of $D_{\perp}$ (fig. 2e)) and their temperature dependence. Then we try to visualize the performance of the different data analysis strategies by showing for each one the error in the observables as the difference between the recovered and the input and data. Thus we have the error obtained on $\langle P_2 \rangle$ (open symbols) and $\langle P_4 \rangle$ (full symbols) (fig. 2b)) and on $D_{\perp}$ (fig. 2f)) by analysing each temperature independently. Similarly in fig. 2c), g) we show the errors obtained when performing a parabolic global target analysis as described in subsect. 4·4. Finally fig. 2d), h) show the residuals corresponding to the HJL global target analysis in subsect. 4·3. We see that this procedure recovers the input data extremely well, showing that the problem can be tackled from a numerical point of view when the true relation existing among the data is correctly guessed. We also notice that

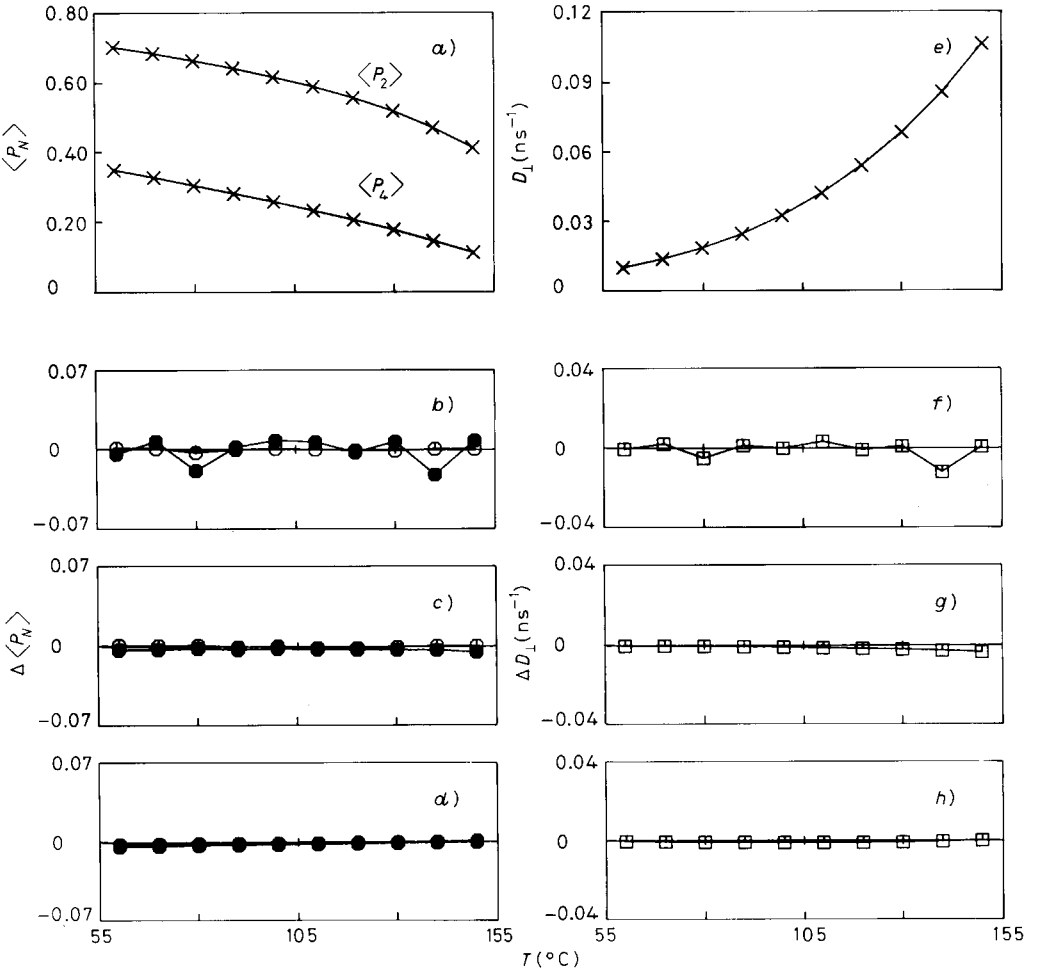

Fig. 2. – Results of a $P_2 - P_4$ analysis of the fluorescence intensities corresponding to a pure P_2 potential. The input values for the second- and fourth-rank probe order parameters $\langle P_2 \rangle$, $\langle P_4 \rangle$ and for the rotational diffusion coefficient $D_\perp$ data are given as the crosses in ((fig. 2*a*), *e*)). The continuous lines help to see the full temperature dependence. The symbols correspond to the difference Δ between recovered and exact results for $\langle P_2 \rangle$ (empty circles), $\langle P_4 \rangle$ (full circles) and for $D_\perp$ (squares) when analysing with individual target analysis (fig. 2*b*), *f*)), parabolic global target analysis (fig. 2*c*), *g*) and with HJL global target analysis (fig. 2*d*), *h*)). The probe transition moments are parallel to the long axis.

$\langle P_2 \rangle$ is always secured quite well for the present conditions. On the other hand, $\langle P_4 \rangle$ and $D_\perp$ are more accurately obtained when a parabolic global target analysis is used. In this case the fourth-rank contribution is also correctly found to be vanishingly small, *i.e.* within no more than 2% of the second-rank one.

We have also investigated the case of the transition moments being both tilted

off from the long axis of an angle θ of 20 degrees ([15]) and we show the results in fig. 3, 4. In this case the analysis is complicated by the fact that reorientation about the long axis modulates the fluorescence depolarization. This in turn implies (cf. eqs. (3), (4)) that correlation functions $\phi_{01}(t)$, $\phi_{02}(t)$ and the component of the rotational diffusion tensor parallel to the rod axis, $D_{\parallel}$, will affect the intensities. It is interesting to see first if we get an indication that new parameters have to be added by analysing the data in a straightforward manner. Thus we started with an individual analysis in terms of a P_2 model with transition moments parallel to the rod axis. The reduced chi square χ^2_r is quite high, varying typically between 1.2 and 1.7, and does suggest the need of a more detailed model. Introduction of θ and $D_{\parallel}$, or rather the ratio $\eta = D_{\parallel}/D_{\perp}$ as parameters in the P_2 model gives a better fit but rather large errors (fig. 3*a*), *c*); 4*a*)) for all the observables. Globalization of $D_{\perp}$ with eq. (11) gives better overall agreement with the input data, as shown in (fig. 3*b*), *d*); 4*b*)). Notice that, if the ITA is repeated with a P_2P_4 model, and the moments fixed parallel to z, a relatively good χ^2_r is obtained, but the parameters recovered are poor. In

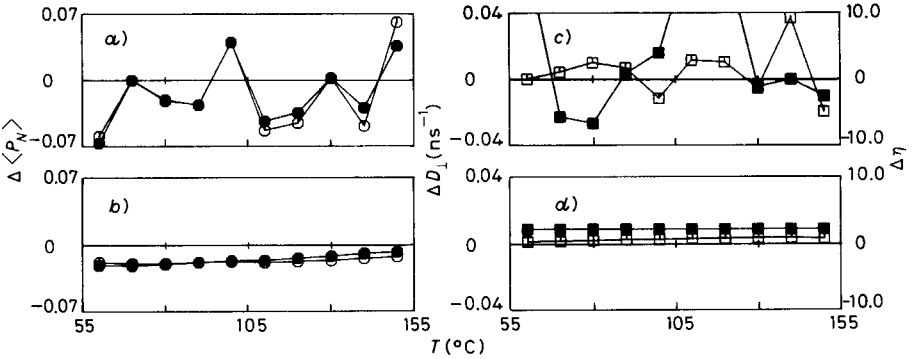

Fig. 3. – Results of the analysis of the fluorescence intensities corresponding to a probe with $\mu \| \bar{\mu}$ and tilted 20° from the rod axis reorienting in a pure P_2 potential. $\langle P_2 \rangle$, $\langle P_4 \rangle$, $D_{\perp}$ and symbol meanings as in fig. 2, while the full squares in fig. 3*c*), *d*) correspond to the rotational diffusion component ratio $\eta = D_{\parallel}/D_{\perp}$. We show results for ITA (fig. 3*a*), *c*)) and for parabolic GT analysis (fig. 3*b*), *d*)). Here $\eta = 10$.

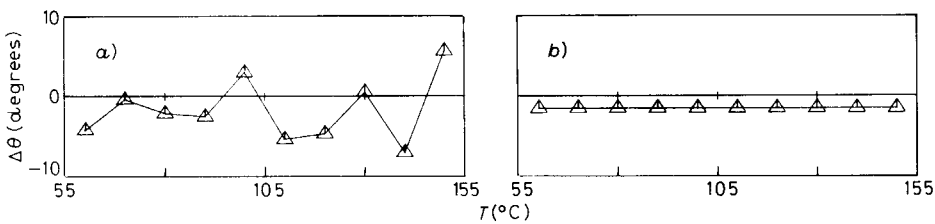

Fig. 4. – Errors in recovering the tilt angle θ (degrees) of the transition moments with respect to the long axis for the case in fig. 3. We show results for ITA (*a*)) and parabolic GT analysis (*b*)).

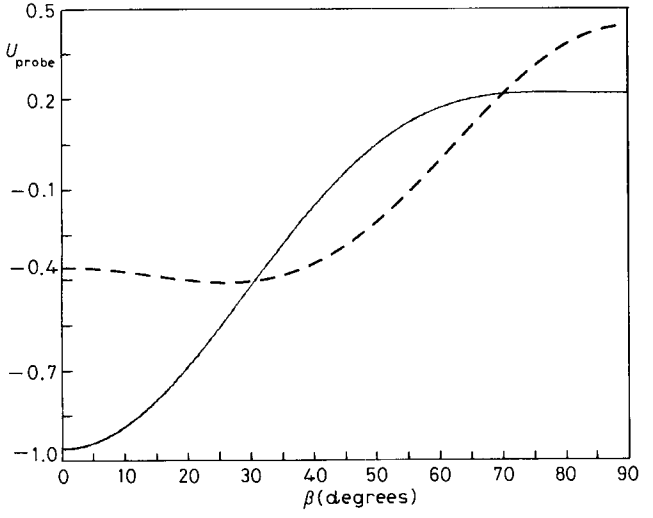

Fig. 5 – The effective probe potential $U_{probe}(\beta)$:

$$-U_{probe}(\beta)/u_2 = \langle P_2\rangle_{solv} P_2(\cos\beta) + (u_4/u_2)\langle P_4\rangle_{solv} P_4(\cos\beta)$$

for $\langle P_2\rangle_{solv} = 0.66$, $\langle P_4\rangle_{solv} = 0.3013$ and $u_4/u_2 = 1$ (continuous line) or -1 (dashed line).

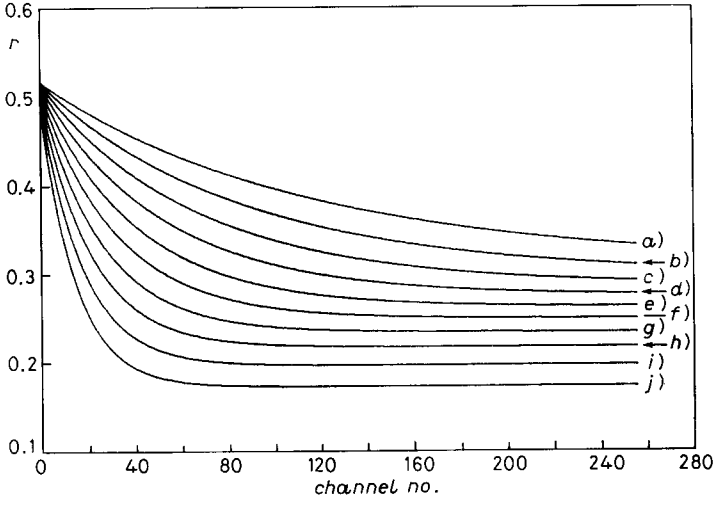

Fig. 6. – Simulated anisotropies $r(t)$ for a rodlike probe with transition moments parallel to the long axis in a $P_2 - P_4$ potential, eq. (9), with coefficients $u_2/k = 800$ K, $u_4/k = 800$ K in a uniaxial nematic with effective potential, eq. (10), and $T_{NI} = 150\,°C$. Curves *a*)-*j*) correspond to temperatures T from 60 °C to 150 °C in steps of 10 °C. Here $D_\perp^0 = 2000\,ns^{-1}$ and $E_a = 31.4$ kJ/mol.

particular, the order parameters $\langle P_2 \rangle$ and $\langle P_4 \rangle$ are systematically underestimated with $\langle P_4 \rangle$ going from 0.2 at the lowest temperature to slightly negative. Thus we conclude that an independent determination of the transition moments is highly recommended if reliable values of the order parameters have to be recovered.

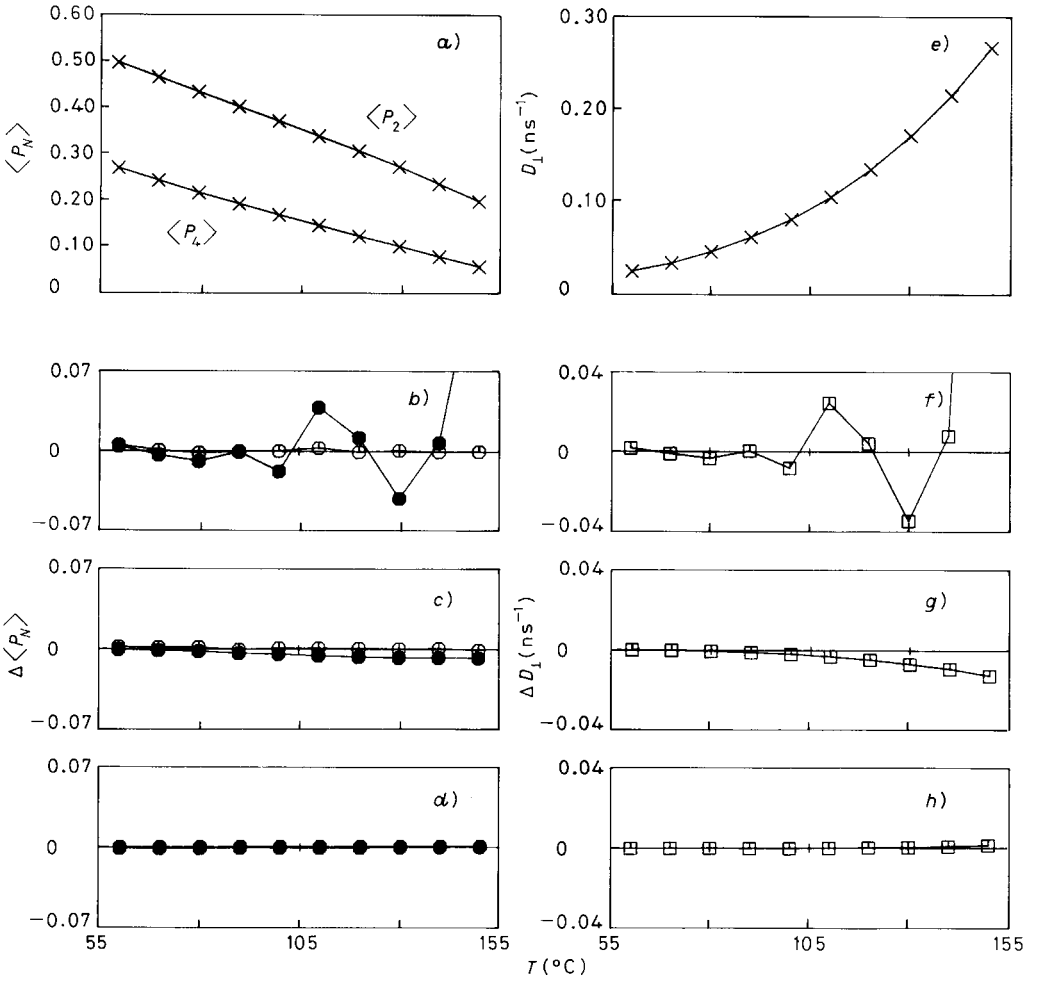

Fig. 7. – Results of an analysis of the fluorescence intensities corresponding to a $P_2 - P_4$ potential as in fig. 6 (continuous lines). The notation for the symbols is the same as in fig. 2. The values obtained with ITA for $\Delta\langle P_4 \rangle$ and $\Delta D_\perp$ at the highest temperature, *i.e.* 0.176 and 0.384 ns^{-1}, are out of scale in fig. 7*b*), *f*).

5·2. *$P_2 - P_4$ potential.* – We now consider a case in which the solute-solvent potential $U_{\text{probe}}(\beta)$ in eq. (9) has both a second-rank and a fourth-rank contributions. The effect of the P_4 term is to make the potential more anisotropic and peaked at $\beta = 0$ if u_4 is positive.

When u_4 is negative, the effect is generally of making the potential less anisotropic, but the combination of the second- and fourth-rank term can also lead to an off axis minimum. Here we have treated both the case of positive and negative u_4 with u_2 and u_4 of equal absolute value. The effective potential acting on the probe is quite different in these two cases, as shown in fig. 5. The first type of potential examined is that with $u_2/k = u_4/k = 800$ K (continuous line in fig. 5). The fluorescence intensities have been calculated as before and lead to anisotropy ratios plotted in fig. 6 for the same set of temperatures used before.

The values of the order parameters and $D_\perp$ corresponding to these anisotropies are reported in fig. 7*a*), *e*). This combination of solute-solvent interaction leads to positive $\langle P_2 \rangle$ and $\langle P_4 \rangle$, but with a temperature dependence less downward concave than usual. In the same figure we also give, in the same format used previously, a comparison of the various kinds of analysis performed. The nonlinear fit to the HJL expression used works very well and the parabolic GTA always performs better than the individual one. In particular the individual analysis in fig. 7*b*), *f*) show a strong correlation between $\langle P_4 \rangle$ and $D_\perp$. Some of the values obtained with the more straightforward ITA are quite wrong. The highest-temperature results, in particular, are out of scale in our plot.

We now move to studying the potential in fig. 5 with $u_2/k = -u_4/k = 800$ K. This is a relatively more difficult case, since curves corresponding to rather different values of the order parameters are more similar than the previous ones, as we see from the anisotropies in fig. 8.

In fig. 9 we show once more the results of an analysis of these simulated data (continuous lines) using individual temperature analysis and global target

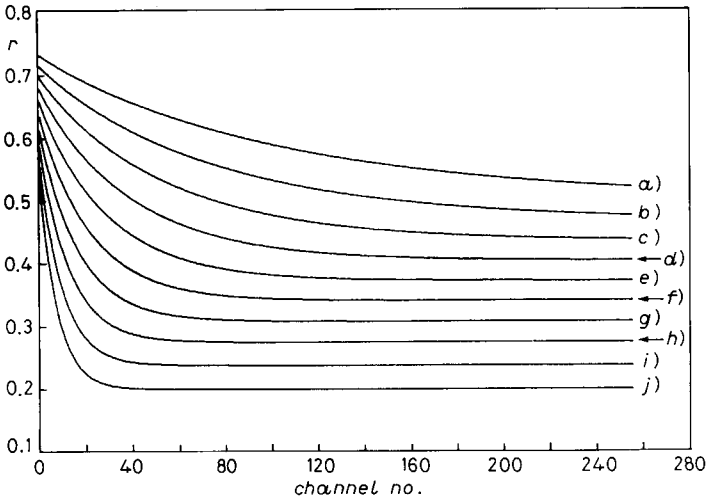

Fig. 8. – Simulated anisotropies for a rodlike probe with transition moments parallel to the long axis in a $P_2 - P_4$ potential, eq. (9), with coefficients $u_2/k = 800$ K, $u_4/k = -800$ K in a uniaxial nematic with effective potential, eq. (10), and $T_{NI} = 150\,°C$. Here $D_\perp^0 = 800\,\text{ns}^{-1}$ and $E_a = 31.4$ kJ/mol. The labelling of the curves is the same of fig. 6.

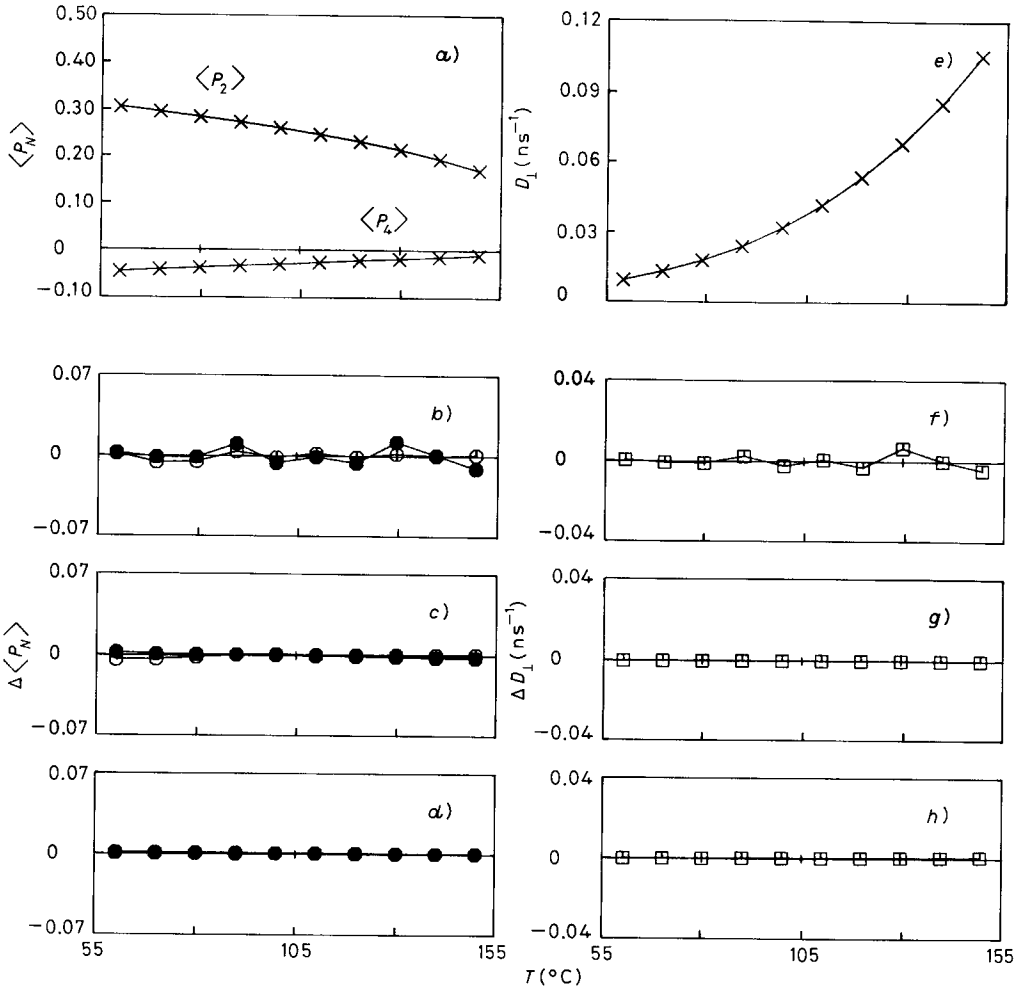

Fig. 9. – Results of the analyses of the fluorescence intensities corresponding to a $P_2 - P_4$ potential as in fig. 8 (continuous lines). The notation for the symbols is the same as in fig. 7.

analysis. As usual we have the temperature dependence of the second-rank and fourth-rank order parameters. We notice that $\langle P_4 \rangle$ exhibits a rather weak temperature dependence and that it is negative in the whole range. All the three analyses shown are quite effective in recovering both order parameters and diffusion coefficient.

5·3. *P_4 potential.* – The limiting case of an effective potential where the P_4 contribution is the largest one is that of a pure P_4 interaction. This model was first studied some years ago using molecular field theory [21] and more recently

[21] C. ZANNONI: *Mol. Cryst. Liq. Cryst. Lett.*, **49**, 247 (1979).

using two-site cluster theory and Monte Carlo simulations [22]. One of the most peculiar findings was that there should exist a temperature interval where the fourth-rank order parameter is bigger than the second-rank one. Various groups have found this behaviour in agreement with fluorescence anisotropy data obtained for 1,6-diphenylhexatriene in DPPC and DMPC membrane vesicles [14,15,23]. Here we consider the probe effective potential as yet another case of eq. (9), this time with $u_2/k = 0\,\mathrm{K}$, $u_4/k = 4000\,\mathrm{K}$. The anisotropic solvent pseudopotential is instead assumed to be described by an ordinary second-rank potential, eq. (10) and $\lambda_{\mathrm{solv}} = 0$. Moreover, we consider transition moments parallel to the long axis and $D_\perp^0$, E_a as given in the caption to fig. 10. In fig. 10 we show the time-dependent anisotropies at the usual series of temperatures.

The order parameters of this solute-solvent interaction are quite interesting. They show $\langle P_4 \rangle$ bigger than $\langle P_2 \rangle$ in the whole temperature range and that $\langle P_2 \rangle$ *vs.* temperature has the unusual characteristic of being upward concave. The intensities have been analysed first with a pure P_2 model and it is gratifying to verify that with this incorrect choice of probe potential completely unacceptable values of χ_r^2 (up to 50) are obtained. An individual target analysis with the P_2P_4 model gives good χ_r^2 and finds the ratio a_2/a_4, which should strictly be zero, to less than 5%. Following this a parabolic GTA analysis has given generally good

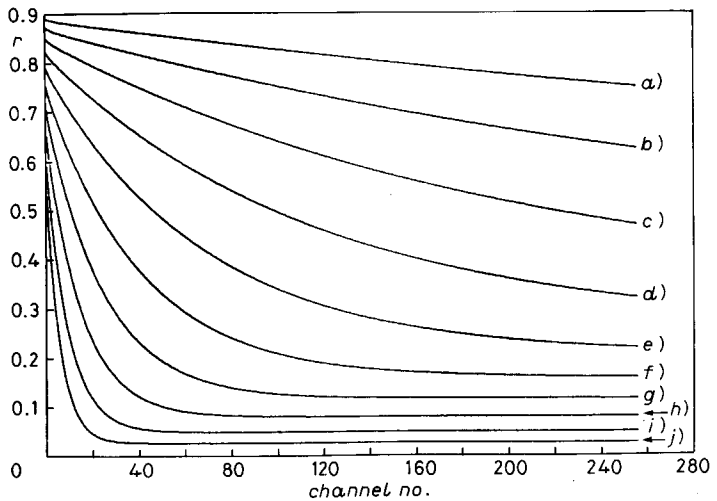

Fig. 10. – Simulated anisotropies for a rodlike probe with transition moments parallel to the long axis probe in a P_4 potential, eq. (9), with coefficients $u_2/k = 0\,\mathrm{K}$, $u_4/k = 4000\,\mathrm{K}$ in a uniaxial nematic with effective potential, eq. (10), and $T_{\mathrm{NI}} = 150\,^\circ\mathrm{C}$. Curves *a*)-*j*) correspond to temperatures T from 60 °C to 150 °C in steps of 10 °C. Here $D_\perp^0 = 4000\,\mathrm{ns}^{-1}$ and $E_a = 31.4\,\mathrm{kJ/mol}$.

---

[22] F. BISCARINI, C. CHICCOLI, P. PASINI and C. ZANNONI: to be published.
[23] H. POTTEL, W. HERREMAN, B. W. VAN DER MEER and M. AMELOOT: *Chem. Phys.*, **102**, 37 (1986).

at least for rodlike probes and monodomain samples. However, it is important that the deconvolution procedure is appropriate. Although the more straightforward technique of analysing each temperature individually (ITA) may be more intuitive and seemingly less biased, this approach is normally inferior to a global target analysis. A good knowledge of the transition moments is also nearly essential. Thus, at this stage, it might be better to concentrate efforts on a few selected reporter molecules, which have a relatively low uncertainty on the orientation of the absorption and emission moments.

* * *

We are grateful to Min. P.I. and C.N.R. for support toward the maintenance costs of the DEC VAX11-780 minicomputer and the FPS-164 array processor used in this work.

APPENDIX

Here we wish to briefly compare the results of a numerical («exact») calculation of the rotational diffusion orientational autocorrelation functions with those obtained from an approximate form in the literature ([13-14]). We have chosen to present for the comparison only one of the second-rank correlation times τ_{mn}, defined as

$$\tau_{mn} = \int_0^\infty \mathrm{d}t \, [\phi_{mn}(t) - \langle P_2 \rangle^2 \delta_{m0} \delta_{n0}], \tag{14}$$

i.e. the long axis correlation time τ_{00}. We recall that this is the only relevant correlation time when both transition moments are parallel to the rod axis. In fig. 12 we show the correlation time generated by the complete numerical solution of the diffusion equation (continuous line) and the approximate ones (dashed lines) ([13]) for positive order parameters and for the $P_2 - P_4$ potential in eq. (8). We show results for the pure P_2 potential limit (curve *A* in fig. 12*a*)) where the approximation works quite well and for a few cases with a nonvanishing P_4 contribution. While the agreement between the approximate curves is also good for $a_4/a_2 = -0.5$, we see that, for a positive P_4 contribution, $a_4/a_2 = 0.5$ (curve *C* in fig. 12*a*)) the agreement worsens. In fig. 12 we show that the approximate expression actually diverges from the correct one when the effective potential acting on the probe is of the pure P_4 type (notice also the different scale on the ordinate). This is due to the double well character of a potential of this kind, which brings, in the limit of very high barrier, a second eigenvalue of the diffusion equation to zero and the corresponding correlation time to diverge. The introduction of a *n-fold* barrier potential in the diffusion equation leads in general to n zero eigenvalues ([24]).

Thus, although in a number of circumstances and particularly for a P_2 model, the approximate expressions work fairly well, we conclude that using them to

([24]) G. MORO and P. L. NORDIO: *Mol. Phys.*, **56**, 255 (1985).

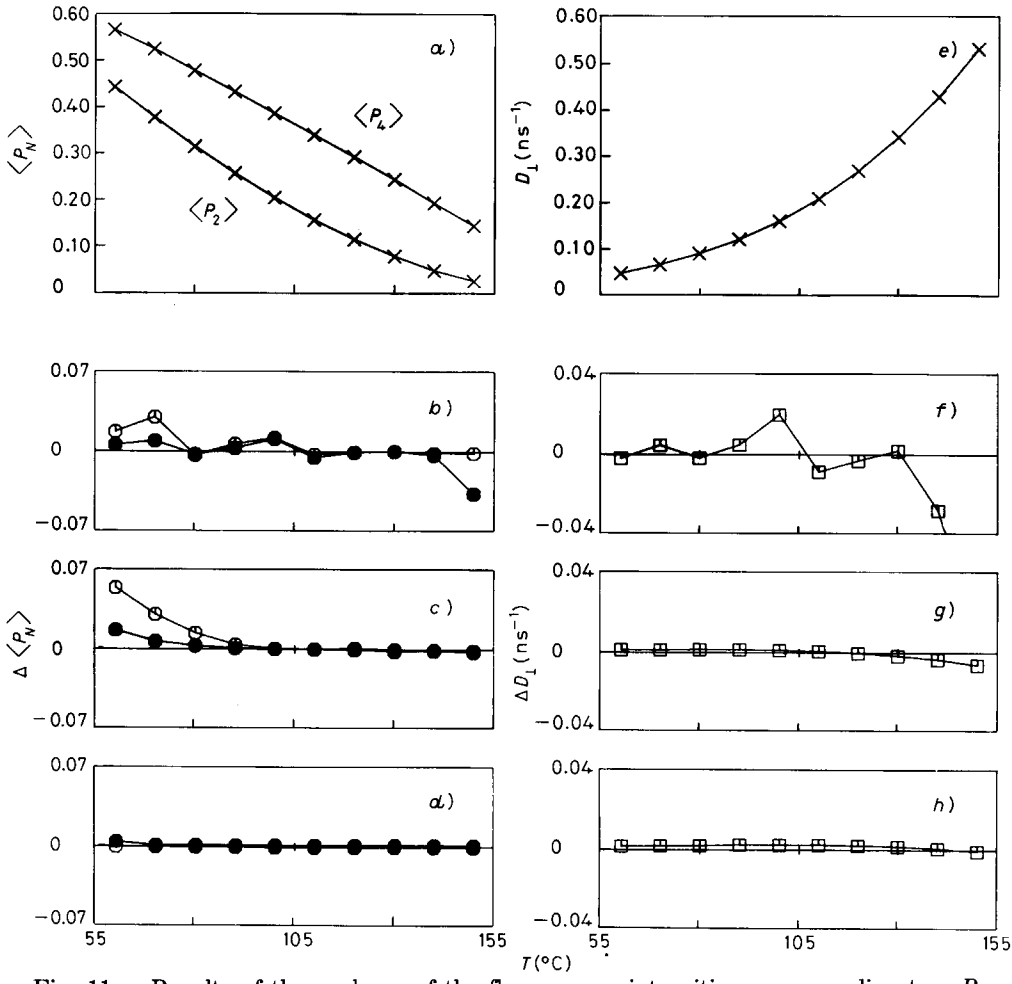

Fig. 11. – Results of the analyses of the fluorescence intensities corresponding to a P_4 potential as in fig. 10 (continuous lines). The notation for the symbols is the same as in fig. 9. The highest temperature value for $\Delta D_\perp$ as found from ITA is -0.084.

results for $D_\perp$, and the order parameters, except at the lowest temperatures used (cf. fig. 11c)). The parameters in eq. (12) are $\lambda_0 = -4.4085$, $\lambda_1 = 0.032\,01$, $\lambda_2 = 0.000\,04$ showing that a parabolic interpolation is more than sufficient to allow for the $a_4(T)$ dependence. The reason for the higher error in this case is probably due to unfavourable fluorescence to reorientation decay range since, as we see from fig. 10, the anisotropy is not fully decayed at the lowest temperature.

6. – Conclusions.

The main conclusion we can draw is that, even though $\langle P_2 \rangle$ is normally recovered better than anything else, $\langle P_4 \rangle$ should also be practically obtainable

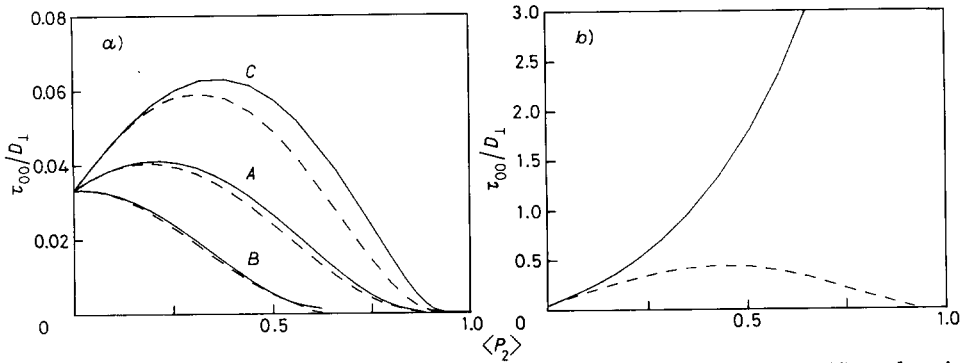

Fig. 12. – A comparison of exact (continuous lines) and approximate ([13]) rod axis correlation time τ_{00} for various $P_2 - P_4$ potentials, eq. (8), as a function of the second-rank order parameter $\langle P_2 \rangle$. We show in fig. 12*a*) results for $a_4/a_2 = 0\,(A)$, $a_4/a_2 = 0.5\,(B)$, $a_4/a_2 = 0.5\,(C)$. In fig. 12*b*) we show the pure P_4 limit results.

analyse experimental data can be dangerous and is not recommended. Indeed it is important that no additional errors are introduced in that case. In particular, since in the approximate expressions (see, *e.g.*, ([13])) an explicit dependence on $\langle P_4 \rangle$ is given, a value for $\langle P_4 \rangle$ is always going to be obtained, even in situations where, maybe, this cannot be reliably done.

● RIASSUNTO

In questo lavoro abbiamo studiato la possibilità di ricavare da un esperimento di depolarizzazione di fluorescenza dipendente dal tempo il parametro d'ordine orientazionale di rango quattro $\langle P_4 \rangle$ per una molecola sonda rodlike disciolta in concentrazione opportuna in un cristallo liquido. A questo scopo sono stati preparati dati simulati a varie temperature, poi analizzati sia individualmente sia simultaneamente usando per la deconvoluzione l'approccio «global target» proposto in precedenza. In particolare è stato esaminato il caso di un potenziale effettivo di tipo $P_4(\cos\beta)$. Sono stati inoltre determinati i limiti di validità di alcune soluzioni approssimate dell'equazione diffusionale recentemente apparse in letteratura.

Можно ли получить $\langle P_4 \rangle$ из деполяризации флуоресценции в жидких кристаллах? I. Стержне-подобные датчики.

Резюме (*). — В этой работе исследуется возможность получения параметра ориентационного порядка четвертого ранга $\langle P_4 \rangle$ для молекулы представляющей стержне-подобный зонд, которая растворена в жидком кристалле, используя эксперимент по деноляризации флуоресценции в зависимости от времени. Подготовлены данные моделирования при различных температурах. Затем эти данные анализируются, используя ранее предложенный подход «Глобальная мишень». В частности, мы исследуем случай эффективного потенциала типа $P_4(\cos\beta)$. Определены пределы применимости некоторых приближенных решений уравнения диффузии, которые недавно появились в литературе.

(*) *Переведено редакцией.*